



Cite this: *Catal. Sci. Technol.*, 2025, 15, 4776

Received 9th April 2025,  
Accepted 14th June 2025

DOI: 10.1039/d5cy00433k

rsc.li/catalysis

## Ligand-assisted nickel catalysis enabling *N,N*-dialkylation and cyclization of acyl hydrazides using aliphatic alcohols†

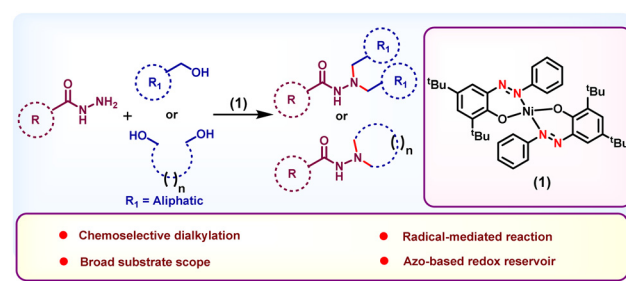
Ayanangshu Biswas, Sourav Mandal, Supriya Halder, Bikramaditya Mandal and Debadis Adhikari \*

Herein, we describe a nickel-catalyzed *N,N*-dialkylation protocol for acyl hydrazides. A series of aliphatic alcohols and diols were successfully dehydrogenated and used for this challenging dialkylation as well as some cyclization reactions. The reaction is chemoselective, as many of the *N,N*-dialkylated products contain an olefinic motif, with the imine linkage selectively reduced while the olefinic one remains intact. The azo-hydrazone redox couple plays a crucial role in the hydrogenation of imines. The reaction proceeds *via* a radical pathway and in striking contrast to previous reports that involve metal hydrides.

The construction of a C–N bond *via* alkylation of an amine has garnered tremendous attention in recent years, owing to the widespread occurrence of substituted amines in natural products, agrochemicals and pharmaceuticals.<sup>1</sup> The conventional methods for C–N bond formation largely conducted the cross-coupling of amines and alkyl halide in the presence of a base, leaving a large amount of waste.<sup>2–5</sup> Replacing the mutagenic alkyl halides by their precursor alcohols might be very effective, although the lower reactivity of alcohols can be a bottleneck. To this end, the conversion of alcohols to carbonyls *via in situ* dehydrogenation, followed by hydrogenation of the resulting imine bond using the borrowed hydrogen from alcohol, has emerged as an appealing method towards C–N bond formation.<sup>6–10</sup> Thus, *N*-alkylation using alcohols as the starting substrates has become a burgeoning field, and a plethora of precious as well as base metal catalysts have been discovered for this purpose.<sup>11–19</sup>

*N,N*-Dialkylated acyl hydrazides can serve as key building blocks in the synthesis of biologically active compounds<sup>20–23</sup> appealing as PG12 agonists,<sup>24</sup> antibacterial,<sup>25</sup> and antifungal agents.<sup>26</sup> Their conventional preparation includes the reaction of acyl halides with substituted hydrazine or the reaction of acyl hydrazides with a stoichiometric amount of strong base, subsequently treating with toxic alkyl halides.<sup>21</sup> All these methods have

pitfalls, including harsh reaction conditions, usage of toxic acyl halides, and generation of copious amounts of waste. The use of simple alcohols to dialkylate acyl hydrazides can be very practical, yet such protocols are scarce. Gunanathan recently established a Ru-Macho catalyst capable of *N,N*-dialkylation and cyclization of acyl hydrazides starting from alcohols.<sup>27</sup> Subsequently, a diaminocyclopentadienone ruthenium tricarbonyl complex and an iridium amidato complex derived from *N*-phenylpicolinamide have also been shown to successfully dialkylate acyl hydrazides using alcohols.<sup>28,29</sup> Notably, there is a severe dearth of base metal catalysts that can perform this challenging reaction, and the sole representative in this direction features a manganese catalyst reported by Balaraman.<sup>30</sup> Nevertheless, the Mn(I) precursor for the catalyst preparation is expensive, which leaves plenty of scope to develop other inexpensive base metal catalysts. Herein, we report the first example of base metal nickel that *N,N*-dialkylates acyl hydrazides



**Scheme 1** Selective catalytic *N,N*-dialkylation of acyl hydrazides using aliphatic alcohols.

Department of Chemical Sciences, Indian Institute of Science Education and Research (IISER) Mohali, Sector-81, Knowledge City, Manauli-140306, India.  
E-mail: adhikari@iisermohali.ac.in

† Electronic supplementary information (ESI) available: Detailed synthetic procedure, control experiments, characterization details, NMR spectra. See DOI: <https://doi.org/10.1039/d5cy00433k>



under relatively mild reaction conditions (Scheme 1). The use of a redox-active azo-phenolate ligand backbone<sup>31</sup> also brings a new mechanistic paradigm that is remarkably different from all prior catalysts used for this purpose. Both dehydrogenation and hydrogenation steps are mediated by a radical pathway that is unprecedented in *N,N*-dialkylation reactions.

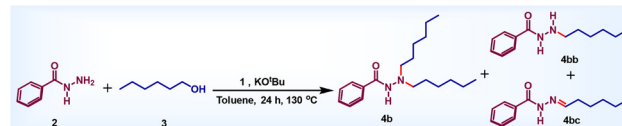
We recently established that a nickel azo-phenolate catalyst, **1** (Scheme 1), is very effective in *N*-alkylation reaction.<sup>32</sup> In addition, it can expand the scope of borrowing hydrogen reactions in *C*-alkylation,<sup>33–35</sup> heterocycle formation<sup>36</sup> or diol cyclization.<sup>37</sup> Our preliminary investigation commenced with the reaction of benzoyl hydrazide with hexanol as the alkylating partner in KO<sup>t</sup>Bu base (Table 1). When the catalytic reaction was performed using 5 mol% of nickel catalyst **1** with 2.2 equiv. of the alcohol in the presence of 0.25 equiv. of KO<sup>t</sup>Bu in toluene, the desired dialkylation product **4b** was isolated in 29% yield, along with a large amount of monoalkylation product **4bb** (42% yield, Table 1). This condition also generated some amount of hydrazone compound **4bc** in 15% yield. However, increasing the base loading to 0.5 equiv. led to the predominant formation of the expected *N,N*-dialkylated product **4b** in 53% yield (entry 2). A further increase in base loading to 1 equiv. improved the formation of **4b** to a commendable 72%, along with a tiny amount of **4bb** and **4bc**. Subsequently, increasing the catalyst loading to 7 mol% significantly augmented the yield of the desired *N,N*-dihexylbenzohydrazide product to 87%. A blank reaction performed in the absence of a catalyst, keeping other reaction conditions identical, did not afford any *N,N*-dialkylated product, although some hydrazone formed. Another control

reaction reveals that the presence of base is critical for the reaction. A solvent screening revealed that xylene afforded **4b** in a 46% yield, while THF did not give any product (entries 7–8). Thus, solvent screening clearly established toluene as the ideal solvent for the reaction.

Other bases, such as KOH and K<sub>2</sub>CO<sub>3</sub> were examined and gave only trace amounts of product, highlighting the efficiency of KO<sup>t</sup>Bu, likely due to its mild reducing character in addition to its basicity (entries 9–10). Bases, such as LDA, LiHMDS, and DBU did not afford any product. Further temperature screening also establishes that the reaction performs well at 130 °C.

Upon achieving the optimized reaction conditions, we next progressed towards exploring the scope of this Ni-catalyzed dialkylation reaction by utilizing an assortment of acyl hydrazide derivatives with an array of aliphatic alcohols as the alkylating partners. Primarily, short-chain aliphatic alcohols, such as pentanol and hexanol were reacted with benzoyl hydrazide to deliver the corresponding dialkylated products **4a** and **4b** in 82–87% yields (Table 2). When the same reaction was performed on a gram scale, **4b** was isolated in 71% yield. Similarly, acyl hydrazides bearing heteroarenes, such as N-containing pyrazinoic acid hydrazide as well as thiophene-2-carbohydrazide, worked well under the current dialkylation protocol, furnishing products *N,N*-dihexyl pyrazinyl hydrazide **4c** and *N,N*-dihexyl thiophenyl hydrazide **4d** in 91% and 69% yields, respectively. Pleasingly, long-chain aliphatic alcohol such as tetradecanol smoothly dialkylated benzoyl hydrazide, synthesizing **4e** in 90% yield. In comparison, 3-phenylpropanol furnished the *N,N*-dialkylated product **4f** in 83% yield.

Table 1 Optimization of reaction conditions



Entry	Catalyst loading	Alcohol (equiv.)	Solvent	Base (mmol)	Yield		
					<b>4b</b>	<b>4bb</b>	<b>4bc</b>
1.	<b>1</b> (5 mol%)	2.2	Toluene	KO <sup>t</sup> Bu (0.25)	29	42	15
2.	<b>1</b> (5 mol%)	2.2	Toluene	KO <sup>t</sup> Bu (0.5)	53	25	17
3.	<b>1</b> (5 mol%)	2.2	Toluene	KO <sup>t</sup> Bu (1)	72	10	8
4.	<b>1</b> (7 mol%)	2.2	Toluene	KO <sup>t</sup> Bu (1)	87	10	n.r.
5.	—	2.2	Toluene	KO <sup>t</sup> Bu (1)	n.r.	n.r.	11
6.	<b>1</b> (7 mol%)	2.2	Toluene	—	n.r.	n.r.	n.r.
7.	<b>1</b> (7 mol%)	2.2	Xylene	KO <sup>t</sup> Bu (1)	46	21	16
8.	<b>1</b> (7 mol%)	2.2	THF	KO <sup>t</sup> Bu (1)	n.r.	n.r.	9
9.	<b>1</b> (7 mol%)	2.2	Toluene	KOH (1)	n.r.	n.r.	12
10.	<b>1</b> (7 mol%)	2.2	Toluene	K <sub>2</sub> CO <sub>3</sub> (1)	n.r.	n.r.	9
11.	<b>1</b> (7 mol%)	2.2	Toluene	KH (1)	n.r.	n.r.	14
12.	<b>1</b> (7 mol%)	2.2	Toluene	NaO <sup>t</sup> Bu (1)	23	36	19
13.	<b>1</b> (7 mol%)	2.2	Toluene	LiHMDS (1)	n.r.	n.r.	9
14.	<b>1</b> (7 mol%)	2.2	Toluene	LDA (1)	n.r.	n.r.	13
15.	<b>1</b> (7 mol%)	2.2	Toluene	DABCO (1)	n.r.	n.r.	n.r.
16.	<b>1</b> (7 mol%)	2.2	Toluene	DBU (1)	n.r.	n.r.	n.r.

Reaction conditions: **1** (x mol %, with respect to benzoyl hydrazide), benzoyl hydrazide (1 mmol), alcohol (2.2 mmol), KO<sup>t</sup>Bu (x mmol), toluene (2 mL), 130 °C, 24 h (isolated yield).

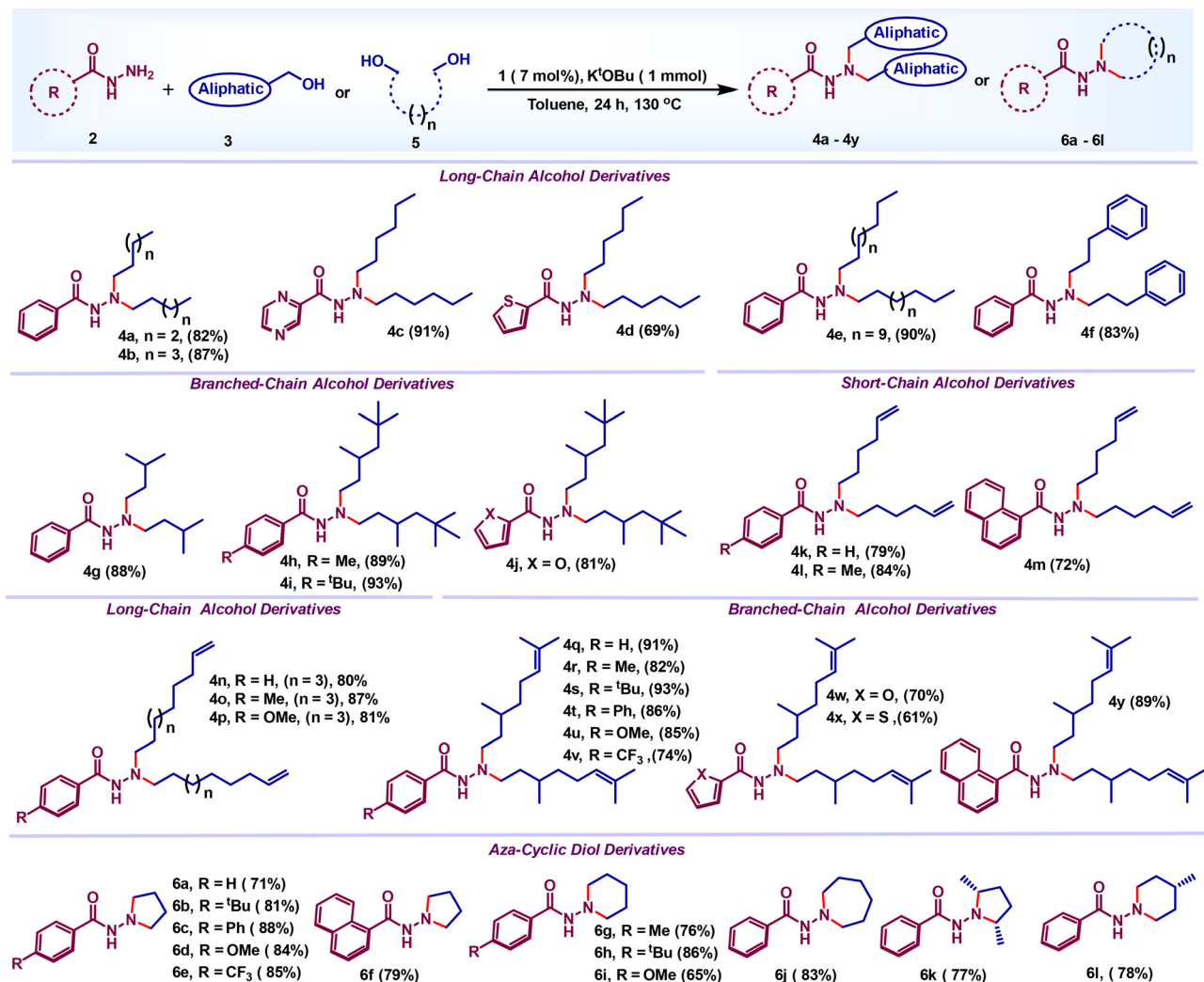


Subsequently, a series of branched-chain alcohols were examined, which reacted smoothly with acyl hydrazides containing electron-donating groups ( $-Me$  and  $-tBu$ ) at the *para* position of the acyl ring to afford products **4h-4i** in 88–93% yields. The furanoyl hydrazide was *N,N*-dialkylated by the proelectrophile 3,5,5-trimethylhexan-1-ol to furnish **4j** in 81% yield, where the Ru-Macho complex provided only the monoalkylated product.<sup>27</sup> Remarkably, this dialkylation protocol hinges on the chemoselective reduction of the imine group, leaving a terminal olefin completely untouched. Accordingly, when hex-5-en-ol and 9-decen-ol were reacted with substituted benzoyl hydrazide and 1-naphthyl hydrazide, the dialkylated products **4k-4p** were isolated in 72–84% yields, preserving the terminal double bond. Other long-chain enol substrates responded well to the reaction conditions to furnish dialkylated products **4n-4p** in 80–87% yields (Table 2). Likewise, citronellol, a sterically hindered unsaturated alcohol, underwent smooth dehydrogenation with various substituted

acyl hydrazides, affording products **4q–4y**. As will be discussed in the mechanistic sketch, the involvement of a radical intermediate in both the dehydrogenation and hydrogenation steps plays a key role in governing the observed chemoselectivity. Encouraged by the excellent efficiency of our catalyst towards dialkylation using acyclic aliphatic alcohol partners, we were intrigued to investigate diols as the alkylating agents, which may lead to intramolecular cyclization. Of note, such cyclic hydrazide motifs are valuable building blocks in drug synthesis.<sup>38</sup> Gratifyingly, 1,4-butandiol was oxidized and successfully cyclized to provide product **6a** in 71% yield. Furthermore, a diverse set of acyl hydrazides bearing electron-donating groups such as  $-\text{Bu}$ ,  $-\text{phenyl}$ , and  $-\text{OMe}$ , as well as electron-withdrawing  $-\text{CF}_3$  groups at the *p*-position of the phenyl ring, reacted with the aforementioned diol to afford the corresponding acyl hydrazide derivatives **6b–6e** in 81–88% yields.

Further, the same alcohol upon treatment with 1-naphthylhydrazide resulted in the formation of **6f** in 79% yield. An

**Table 2** Substrate scope for *N,N*-dialkylation and cyclization reactions



Reaction conditions: acylhydrazide (1 mmol), primary alcohol (2.2 mmol),  $\text{KO}^\text{t}\text{Bu}$  (1 mmol), **1** (7 mol%), toluene (2 mL), 130 °C, 24 h. When diol was the substrate, 1.2 mmol was used.

analogous reaction of 1,5 pentanediol with different benzoyl hydrazide substrates yielded the corresponding 6-membered cyclic products (**6g–6i**) in good yields. Analogously, 1,6 hexanediol smoothly prepared the seven-membered cyclized product **6j** in 83% yield. Next, we interrogated whether substituted diols can also be an efficient substrate for such cyclization reactions. Interestingly, 2,5-hexanediol and 3-methylpentane-1,5-diol smoothly reacted with benzoyl hydrazide, furnishing the corresponding cyclized products **6k** and **6l** in 77 and 78% yields, respectively.

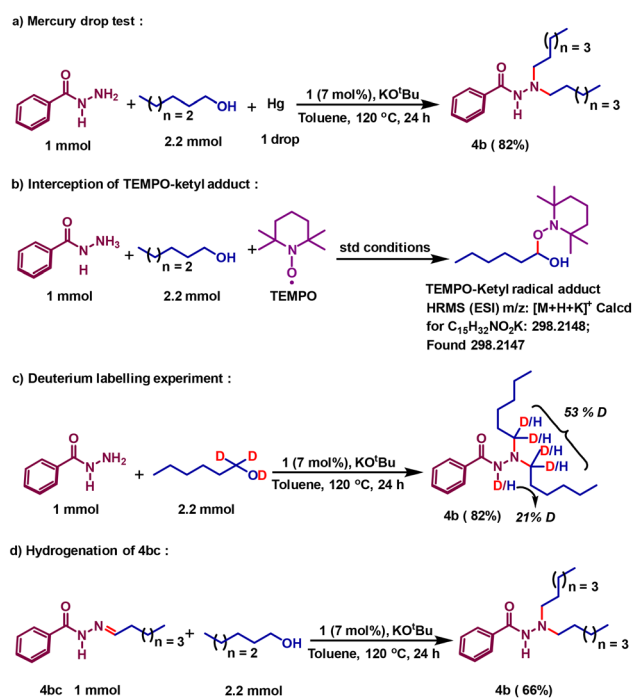
Upon establishing a successful dialkylation protocol, we were interested to delineate the mechanistic sketch of the reaction. It is very intriguing that the reaction involves radical intermediates, and the dehydrogenation steps are strikingly different from prior catalysts, where metal hydride formation was imminent.<sup>27,29,39</sup> Earlier we described the explicit details of alcohol dehydrogenation and showed how a radical centralized in the azo motif can facilitate the critical hydrogen atom transfer (HAT) step to conduct smooth dehydrogenation reactions.<sup>31,32</sup> We have also shown clearly that upon dehydrogenation, the azo motif is converted to a hydrazo species,  $1^{\text{H},\text{H}}$ , so that two-electron oxidation of a substrate alcohol is concomitant with two-electron reduction of the azo motif present in the catalyst molecule. Aliphatic alcohols are also dehydrogenated by the same pathway that we have proved recently *via* a Bell–Evans–Polanyi analysis.<sup>31</sup> In the current mechanistic investigation, we will use 1-hexanol as the model aliphatic alcohol and delineate how two alkyl units are introduced to alkylate the terminal nitrogen of the benzoyl hydrazide. Initially, we attempted to prove the homogeneous nature of the catalytic reaction by performing a mercury drop test, which did not have any negative impact on the reaction (Scheme 2a). In strong support of our radical mechanism, where an azo-promoted HAT generates a ketyl radical, we intercepted such a radical intermediate. The TEMPO-adduct of the ketyl radical from 1-hexanol was detected by ESI high-resolution mass spectrometry (Scheme 2b).

To prove that the process undergoes a borrowing hydrogen method, we further conducted a deuterium labelling experiment. Starting with  $\alpha$ -dideuterated 1-hexanol, the deuterium incorporation at the designated carbons in product **4b** was proved (Scheme 2c). Upon dehydrogenation, a hexanal forms, which condenses with benzoyl hydrazide to afford the imine intermediate **4bc**. To prove the involvement of this intermediate, it was synthesized separately and hydrogenated using 1-hexanol in the presence of catalyst **1**. Such a control reaction affords the desired dialkylated product **4b** in 66% yield (Scheme 2d) along with the isolation of dehydrogenated byproduct hexanal in 57% yield. For the hydrogenation of the imine bond, the hydrogen stored at the hydrazo motif is used, adopting a radical mechanism. The details of radical-promoted imine hydrogenation during the monoalkylation was proved earlier.<sup>40</sup> In this current work,

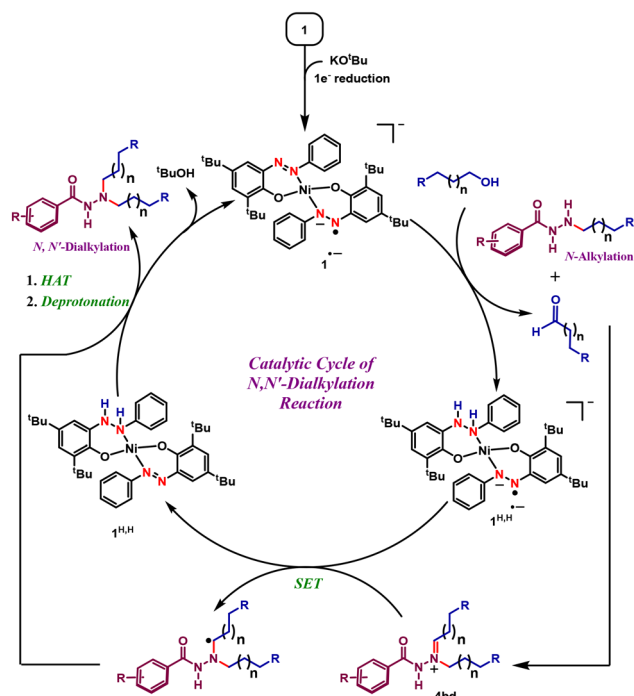
we will describe how that second alkylation proceeds, notably *via* the involvement of the radical intermediate. Intuitively, the mono-alkylated product further condenses with hexanal to give **4bd** as the intermediate (Scheme 3). The nickel catalyst, upon conducting dehydrogenation, remains as  $1^{\text{H},\text{H}^-}$ , where one of the azo-arms is mono-reduced. During C-alkylation reactions, we have shown that this electron is passed to the enone substrate and reduces it, and such a reduced intermediate conducts further HAT.<sup>37</sup> Along the same line, the iminium intermediate **4bd** can be mono-reduced, and this reduction is even more plausible given the cationic nature of the substrate.

In the context of chemoselectivity, it is clear that the iminium cation is reduced much faster than the isolated double bond, ensuring selective reduction of the imine over olefin.

The easy generation of the radical on the imine or iminium cation by single electron reduction facilitates the hydrogenation, leaving the terminal olefin untouched. Once reduced by a single electron, the resulting carbon-centered radical facilitates a HAT step from the hydrazo motif. The dialkylated product is released upon HAT, while the catalyst N–H is deprotonated by  $\text{KO}^{\text{t}}\text{Bu}$  so that the mono-reduced form of the catalyst is regenerated (Scheme 3). This catalytic intermediate,  $1^{\text{--}}$  starts the next round of alcohol dehydrogenation. Notably, all prior literature describing transition metal-catalyzed hydrogen autotransfer invoked a metal hydride.<sup>41–43</sup> Usually, a  $\beta$ -hydride elimination from a metal-bound alkoxide generates the metal hydride. These findings clearly demonstrate the utility of the redox-



**Scheme 2** Control reactions to mechanistically probe the *N,N*-dialkylation protocol.



**Scheme 3** Plausible radical-mediated mechanistic cycle highlighting iminium hydrogenation.

responsive ligand backbone, which can store the reducing equivalent.<sup>44–46</sup> This way, it provides an orthogonal avenue for conducting smooth (de)hydrogenation reactions to yield the final *N,N*-dialkylation product.

## Conclusions

In summary, we describe an efficient *N,N*-dialkylation protocol using a nickel catalyst where the redox-active azo ligand plays an extremely important role in steering both dehydrogenation and hydrogenation steps. The efficiency of the catalyst in dehydrogenating aliphatic diols was obvious, as the long aliphatic chains were installed on amine nitrogen to achieve dialkylation. A series of products comprising a long aliphatic straight chain, a branched chain, and an olefinic motif at the terminal position of the chain have been successfully synthesized in high yields using this simple catalyst. The catalyst also showcases excellent chemoselectivity by preferentially reducing the imine bonds over the olefinic bonds. Both critical steps for the reaction—the dehydrogenation of alcohol and the hydrogenation of iminium cation—are driven by a radical mechanism. During imine hydrogenation, a radical housed in the azo ligand is transported to monoreduce such substrate, which subsequently performs HAT from the hydrazo of the ligand framework. Thus, two azophenolates present in the ligand scaffold behave as a redox reservoir, switch between azo-hydrazo redox shuttle, and operate in a very cooperative fashion to conduct this reaction successfully. We hope the catalytic efficiency of the present

system shows promise for future BH catalyst design, where redox-active ligands can play an increasingly important role.

## Experimental section

All starting materials utilized in this study were procured from commercial suppliers. Potassium *tert*-butoxide, potassium hydroxide, potassium carbonate, and sodium hydroxide were purchased from Avra Synthesis Pvt. Ltd., India. Primary and secondary alcohols were purchased from TCI (India) and BLD Pharma. Fluorene was purchased from BLD Pharma. All these chemicals were used without further purification. Glassware was dried overnight at 160 °C. Solvents such as acetonitrile, ethanol, and dichloromethane were used as received (Finar Chemicals). Toluene was dried by heating over sodium with benzophenone as an indicator. For thin-layer chromatography (TLC), aluminum foil coated with silica and a fluorescent indicator @254 nm (from Merck) was used. Column chromatography was performed using SD Fine silica gel (100–200 mesh) using a gradient of hexane and diethyl ether as the mobile phase.

## Analytical information

All synthesized products were isolated and characterized by <sup>1</sup>H and <sup>13</sup>C NMR spectroscopy and high-resolution mass spectrometry. IR spectra were recorded on a Perkin-Elmer FTIR spectrometer using KBr pellets. <sup>1</sup>H NMR and <sup>13</sup>C NMR spectra were recorded on a 400 MHz Bruker Biospin Advance III FT-NMR spectrometer. NMR shifts were reported as delta ( $\delta$ ) units in parts per million (ppm), and coupling constants ( $J$ ) were reported in hertz (Hz). Chemical shifts ( $\delta$ ) were quoted to the nearest 0.01 ppm relative to the residual protons in CDCl<sub>3</sub> ( $\delta$  7.26 ppm). Carbon chemical shifts were internally referenced to the deuterated solvent signal of CDCl<sub>3</sub> ( $\delta$  77.1 ppm). <sup>13</sup>C NMR data were proton decoupled. High-resolution mass spectra (HRMS) were recorded on a Waters QTOF mass spectrometer. For chlorine-containing molecules, the most abundant <sup>35</sup>Cl was considered for the monoisotopic mass calculation.

## Synthesis of 1

The azo-phenolate ligand was synthesized using a previously reported procedure.<sup>32</sup> In a 100 mL round-bottom flask, a methanolic solution of azo-phenolate ligand (0.1 mmol) and an equimolar amount of KOH were added, and the mixture was stirred at room temperature for 30 min. Next, Ni(OAc)<sub>2</sub> (0.05 mmol) was added, and the reaction mixture was further refluxed for another 30 min, during which precipitation was observed. After completion of the reaction, the solution was filtered, affording a dark brown-colored compound **1** in 82% yield. The desired product was fully characterized by <sup>1</sup>H and <sup>13</sup>C NMR and IR spectroscopy.



**Synthesis of  $1^{\text{H},\text{H}}$** 

In a 25 mL Schlenk flask, equimolar quantities of **1**, benzyl alcohol and KO<sup>t</sup>Bu (1 mmol each) were added, and the flask was connected to a condenser under a nitrogen flow. The solution was heated to reflux for 4 h, after which the color changed to maroon. The reaction mixture was dried *in vacuo*, and the crude mixture was washed with dry hexane (5 mL × 3). The precipitate was dried to collect **1<sup>H,H</sup>** in 68% yield. The desired product was fully characterized by <sup>1</sup>H, <sup>13</sup>C NMR and IR spectroscopy.<sup>36</sup>

**General procedure for *N,N*-dialkylation of acyl hydrazides**

In a typical reaction, a 15 mL pressure tube was charged with **1** (7 mol%), KO<sup>t</sup>Bu (1 mmol), alcohols (2.2 mmol), and substituted acylhydrazide (1 mmol), along with 2 mL toluene. The reaction flask was purged with an inert gas for a few minutes before closing the flask tightly. The reaction mixture was stirred at 130 °C for 24 h. The reaction mixture was cooled to room temperature upon completion of the reaction and concentrated *in vacuo*. The residue was purified by column chromatography using hexane/diethyl ether as an eluent to afford pure products. The desired products were fully characterized by <sup>1</sup>H and <sup>13</sup>C NMR spectroscopy.

**Data availability**

All data required for the report are available in the form of ESI.†

**Conflicts of interest**

There is no conflict of interest to declare.

**Acknowledgements**

We thank STARS-2 (MHRD), India (Grant No. STARS-2/2023/474), and IISER Mohali for financial support. The authors further thank the IISER Mohali central facility for analytical data.

**References**

- J. Magano and J. R. Dunetz, *Chem. Rev.*, 2011, **111**, 2177–2250.
- S. Lee, M. Jørgensen and J. F. Hartwig, *Org. Lett.*, 2001, **3**, 2729–2732.
- X. Huang and S. L. Buchwald, *Org. Lett.*, 2001, **3**, 3417–3419.
- B. P. Fors and S. L. Buchwald, *J. Am. Chem. Soc.*, 2010, **132**, 15914–15917.
- X.-B. Lan, Y. Li, Y.-F. Li, D.-S. Shen, Z. Ke and F.-S. Liu, *J. Org. Chem.*, 2017, **82**, 2914–2925.
- M. H. S. A. Hamid, C. L. Allen, G. W. Lamb, A. C. Maxwell, H. C. Maytum, A. J. A. Watson and J. M. J. Williams, *J. Am. Chem. Soc.*, 2009, **131**, 1766–1774.
- P. Piehl, M. Peña-López, A. Frey, H. Neumann and M. Beller, *Chem. Commun.*, 2017, **53**, 3265–3268.
- G. E. Dobereiner and R. H. Crabtree, *Chem. Rev.*, 2010, **110**, 681–703.
- C. Gunanathan and D. Milstein, *Science*, 2013, **341**, 249–260.
- M. Siddique, B. Boity and A. Rit, *Catal. Sci. Technol.*, 2023, **13**, 7172–7180.
- R. Grigg, T. R. B. Mitchell, S. Sutthivaiyakit and N. Tongpenyai, *J. Chem. Soc., Chem. Commun.*, 1981, 611–612, DOI: [10.1039/C39810000611](https://doi.org/10.1039/C39810000611).
- G. Guillena, D. J. Ramón and M. Yus, *Chem. Rev.*, 2010, **110**, 1611–1641.
- T. Irrgang and R. Kempe, *Chem. Rev.*, 2019, **119**, 2524–2549.
- B. G. Reed-Berendt, D. E. Latham, M. B. Dambatta and L. C. Morrill, *ACS Cent. Sci.*, 2021, **7**, 570–585.
- K. Das, A. Mondal, D. Pal and D. Srimani, *Org. Lett.*, 2019, **21**, 3223–3227.
- D. Bhattacharyya, P. Adhikari, K. Deori and A. Das, *Catal. Sci. Technol.*, 2022, **12**, 5695–5702.
- P. Daw, A. Kumar, N. A. Espinosa-Jalapa, Y. Ben-David and D. Milstein, *J. Am. Chem. Soc.*, 2019, **141**, 12202–12206.
- S. Elangovan, J. Neumann, J.-B. Sortais, K. Junge, C. Darcel and M. Beller, *Nat. Commun.*, 2016, **7**, 12641.
- K. Das, A. Mondal, D. Pal, H. K. Srivastava and D. Srimani, *Organometallics*, 2019, **38**, 1815–1825.
- P. Majumdar, A. Pati, M. Patra, R. K. Behera and A. K. Behera, *Chem. Rev.*, 2014, **114**, 2942–2977.
- U. Ragnarsson, *Chem. Soc. Rev.*, 2001, **30**, 205–213.
- S. N. Mali, B. R. Thorat, D. R. Gupta and A. Pandey, *Eng. Proc.*, 2021, **11**, 21.
- A. Shamsabadi and V. Chudasama, *Org. Biomol. Chem.*, 2017, **15**, 17–33.
- N. Hamanaka, K. Takahashi, Y. Nagao, K. Torisu, S. Shigeoka, S. Hamada, H. Kato, H. Tokumoto and K. Kondo, *Bioorg. Med. Chem. Lett.*, 1995, **5**, 1087–1090.
- H. M. Eisa, A. S. Tantawy and M. M. el-Kerdawy, *Pharmazie*, 1991, **46**, 182–184.
- N. T. Thu-Cuc, N. P. Buu-Hoï and N. D. Xuong, *J. Med. Pharm. Chem.*, 1961, **3**, 361–367.
- S. Thiagarajan and C. Gunanathan, *Org. Lett.*, 2020, **22**, 6617–6622.
- W.-H. Wang, W.-Y. Shao, J.-Y. Sang, X. Li, X. Yu, Y. Yamamoto and M. Bao, *Organometallics*, 2023, **42**, 2623–2631.
- N. Joly, L. Bettioni, S. Gaillard, A. Poater and J.-L. Renaud, *J. Org. Chem.*, 2021, **86**, 6813–6825.
- R. Babu, S. S. Padhy, G. Sivakumar and E. Balaraman, *Catal. Sci. Technol.*, 2023, **13**, 2763–2771.
- R. Singh, A. K. Bains, A. Kundu, H. Jain, S. Yadav, D. Dey and D. Adhikari, *Organometallics*, 2023, **42**, 1759–1765.
- A. K. Bains, A. Kundu, S. Yadav and D. Adhikari, *ACS Catal.*, 2019, **9**, 9051–9059.
- A. Biswas, A. K. Bains and D. Adhikari, *Catal. Sci. Technol.*, 2022, **12**, 4211–4216.
- A. K. Bains, A. Biswas, A. Kundu and D. Adhikari, *Adv. Synth. Catal.*, 2022, **364**, 2815–2821.
- A. K. Bains, A. Biswas and D. Adhikari, *Adv. Synth. Catal.*, 2022, **364**, 47–52.



36 A. K. Bains, V. Singh and D. Adhikari, *J. Org. Chem.*, 2020, **85**, 14971–14979.

37 A. K. Bains, A. Kundu, D. Maiti and D. Adhikari, *Chem. Sci.*, 2021, **12**, 14217–14223.

38 M. Ślusarezyk, W. M. De Borggraeve, G. Hoornaert, F. Deroose and J. T. M. Linders, *Eur. J. Org. Chem.*, 2008, **2008**, 1350–1357.

39 A. Kaithal, B. Chatterjee, C. Werlé and W. Leitner, *Angew. Chem., Int. Ed.*, 2021, **60**, 26500–26505.

40 A. K. Bains, A. Kundu, R. Singh, H. Jain and D. Adhikari, *Eur. J. Inorg. Chem.*, 2024, **27**, e202400558.

41 S. Fu, Z. Shao, Y. Wang and Q. Liu, *J. Am. Chem. Soc.*, 2017, **139**, 11941–11948.

42 K. Sarkar, K. Das, A. Kundu, D. Adhikari and B. Maji, *ACS Catal.*, 2021, **11**, 2786–2794.

43 M. Bertoli, A. Choualeb, A. J. Lough, B. Moore, D. Spasyuk and D. G. Gusev, *Organometallics*, 2011, **30**, 3479–3482.

44 V. Lyaskovskyy and B. de Bruin, *ACS Catal.*, 2012, **2**, 270–279.

45 K. Singh, A. Kundu and D. Adhikari, *ACS Catal.*, 2022, **12**, 13075–13107.

46 J. I. van der Vlugt, *Chem. – Eur. J.*, 2019, **25**, 2651–2662.

